Article

Journal of Vibration and Control
2019, Vol. 25(1) 132–140

DOI: 10.1177/1077546318772256
journals.sagepub.com/home/jvc
SAGE

Nonlinear dynamics and robust control of sloshing in a tank

Tingting Zhang and Jianying Yang

Abstract

Sloshing is a complex nonlinear dynamic phenomenon which has a significant influence on the stability of structure–fluid systems. In this study, the dynamic equation of sloshing based on Hamilton principle is established and linearized into a state space equation. Considering the uncertainty of the system, a robust H infinite guaranteed cost control method is proposed to mitigate the response of fluid wave height to horizontal acceleration of the tank body. Simulation results are given to demonstrate the closed-loop performance of the nonlinear dynamic modeling and linear optimal control method.

Keywords

Sloshing, nonlinear dynamics, Hamilton principle, guaranteed cost control

1. Introduction

Liquid tanks exist in many mechanical systems and play a dispensable role in modern industry and frontier science fields, such as oil storage tanks, liquefied natural gas storage tanks, and liquid rocket fuel tanks. Free-surface motions of liquid under gravity in tanks are of practical importance. The motion of liquid free surface is defined as sloshing. For sloshing in the vertically excited tank, the free surface exhibits nonlinear behavior.

The sloshing problem in a tank has an important application prospect, which not only has the general characteristics of free surface flow, but also interacts strongly with the container that limits its motion. It is known that partially filled tanks are prone to violent sloshing under certain motions. The large liquid movement creates highly localized impact pressure on tank walls, which may in turn cause structural damage and may even create sufficient moment to affect the stability of the vehicle which carries the container. Further applications in the aerospace industry are described by Abramson (1966).

Many numerical studies have been undertaken into sloshing in fixed and moving tanks. For example, Telste (1985) modeled the time-dependent behavior of the free surface of an inviscid liquid in a two-dimensional (2D) tank by means of a finite difference model. Ferrant and Le Touze (2001) applied an inviscid pseudo-spectral model to predict three-dimensional (3D) sloshing motions. Yue (2005) studied 3D large amplitude liquid sloshing in a cylindrical open tank under pitching excitations using the arbitrary Lagrange–Euler description. Takashi et al. (2012) investigated nonlinear responses of surface waves in rigid square and nearly square tanks partially filled with liquid subjected to obliquely horizontal, sinusoidal excitation theoretically and experimentally. Love and Tait (2014) developed and experimentally validated a model to describe the structure–tuned liquid damper (TLD) interaction of a 2D system when the TLD tank geometry is complex.

Venugopal and Bernstein (1996) considered two possible active control methods for attenuating the response of the fluid to an external disturbance acceleration acting on the tank. The first method uses surface pressure control, whereas the second method uses a flap actuator on the surface of the fluid. In the paper by Bandyopadhyay et al. (2009), the problem of

State Key Laboratory for Turbulence and Complex Systems, Department of Mechanics and Engineering Science, Peking University College of Engineering, Beijing, China

Received: 22 November 2017; accepted: 21 March 2018

Corresponding author:
Jianying Yang, State Key Laboratory for Turbulence and Complex Systems, Department of Mechanics and Engineering Science, Peking University College of Engineering, Beijing 100871, China.
Email: yjy@pku.edu.cn

the control of slosh has also been considered. A simple pendulum model is considered to represent the lateral slosh. Coupled slosh dynamics yielded a second order under-actuated system. Partial feedback linearization was used. A high-gain sliding mode observer was proposed to estimate the states.

In the work of De Souza and de Souza (2014), the slosh dynamics was modeled using a common pendulum model and it was considered to be unactuated. The control inputs were defined by a transverse body fixed force and a moment about the center of mass. A comparative investigation designing the satellite attitude control systems by the linear quadratic regulator (LQR) and linear quadratic Gaussian methods was done. Zang and Huang (2015) designed a command smoothing technique to suppress slosh for the two fundamental and high modes. Comparing with the combined input shaper and the low-pass filter scheme, the presented smoother provided more robustness to variations in the sloshing frequency.

The present paper describes a fully nonlinear numerical model of liquid sloshing motion in a vertically excited rectangular tank using analytical dynamic methods. It is assumed that the liquid is inviscid, incompressible, and irrotational, that the free surface does not become vertical or overturn, and that surface tension can be neglected. The unity of fluid motion and rigid body motion is realized by the application of Hamilton principle. Separation of variables is employed to derive the state space model of motion for several sloshing modes. A robust H infinite guaranteed cost control method considering the uncertainty of the system is proposed and conducted in order to attenuate the response of wave height to external excitations. Simulation results are also given to validate the control ability and demonstrate the difference between this method and others.

In the next section the sloshing model is described by system dynamics and boundary conditions. Then in Section 3, by separation of variables and reasonable simplification, the partial differential dynamic equations are linearized. State space models are built for low sloshing modes after high-order modal truncation. Next, the feedback controller based on robust H infinite guaranteed cost control is presented in Section 4, which is followed by simulation results in Section 5. Concluding remarks are given in the final section.

2. Model description

2.1. System dynamics

Liquid sloshing system is composed of a discrete system (the rigid body) and continuous medium (the liquid). Although the modeling of liquid movement is based on Euler equations of fluid dynamics, which is different from that of rigid bodies, a uniform modeling method can be applied using analytical mechanics when the liquid is regarded as a set of special particles (Liu, 2015).

Consider a rigid rectangular tank with a cross-section area of width multiples by breadth $a \times b$, as shown in Figure 1. The tank is partially filled with liquid to the depth of h. The Cartesian coordinate system Oxy is established with its origin in the center of the undisturbed free surface and the plane Oxy coincides with the surface.

The liquid elevation at position (x, y) is designated by $\eta(x, y, t)$. The liquid is assumed to be ideal (uniform, inviscid, and incompressible) in the following theoretical analysis so that the velocity potential $\phi(x, y, z, t)$ can be introduced in order to represent the relative liquid motion to the tank. For ideal fluid, the velocity potential $\phi(x, y, z, t)$ satisfies Laplace's equation, which is expressed as

$$\frac{\partial^2 \phi}{\partial x^2} + \frac{\partial^2 \phi}{\partial y^2} + \frac{\partial^2 \phi}{\partial z^2} = 0 \tag{1}$$

The Lagrangian function of the sloshing system can be expressed as

$$L = T - V \tag{2}$$

where T and V represent the kinetic energy and potential energy of the system, respectively, and can be given

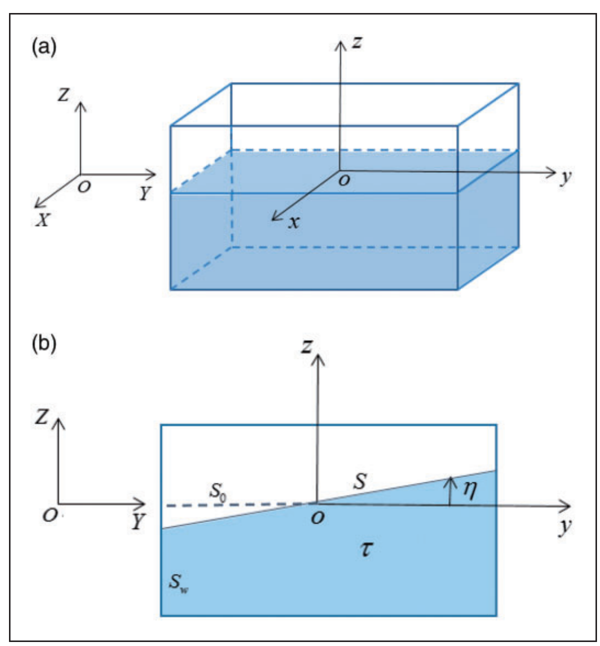

Figure 1. Tank partially filled with liquid: (a) three-dimensional graph and (b) side view graph.

by (Chen et al., 2005)

$$T = \frac{1}{2} M\dot{\mathbf{U}}^2 + \frac{1}{2}\rho \int_\tau (\nabla\phi)^2 \mathrm{d}\tau \tag{3}$$

$$V = \frac{1}{2}\rho g \int_S \eta^2 \mathrm{d}S \tag{4}$$

where U, ρ, and g represent the displacement of tank, the fluid density, and the gravitational acceleration, respectively.

Substitution of equations (3) and (4) into the reformative Hamilton principle gives

$$\int_0^t \left(\delta T - \delta V + \int_\tau p \mathrm{div}\delta\mathbf{r} \mathrm{d}\tau \right) \mathrm{d}t = 0 \tag{5}$$

$$\begin{aligned} &\int_0^t (\delta T - \delta V)\mathrm{d}t \\ &= \int_0^t \left(M\dot{\mathbf{U}}\delta\dot{\mathbf{U}} + \rho \int_\tau \nabla\phi\delta\nabla\phi \mathrm{d}\tau - \rho g \int_S \eta\delta\eta \mathrm{d}S \right) \mathrm{d}t \end{aligned} \tag{6}$$

$$\begin{aligned} \rho \int_\tau \nabla\phi \cdot \delta\nabla\phi \mathrm{d}\tau = &\frac{\mathrm{d}\mathbf{Q}}{\mathrm{d}t}\delta\mathbf{U} \\ &+ \rho \int_\tau \nabla\left(\frac{\partial\phi}{\partial t} + \frac{1}{2}\nabla\phi \cdot \nabla\phi \right) \cdot \delta\mathbf{r} \mathrm{d}\tau \end{aligned} \tag{7}$$

where Q represents the momentum of liquid, v is the absolute velocity of liquid particle, and r is the relative displacement vector of the particle, which satisfies

$$\mathbf{r} \cdot \mathbf{n} = \eta \tag{8}$$

Based on the incompressible condition of the liquid, according to the divergence theorem, it can be obtained that

$$\int_\tau p \mathrm{div}\delta\mathbf{r}\mathrm{d}\tau = \int_S p\mathbf{n} \cdot \delta\mathbf{r}\mathrm{d}S - \int_\tau \nabla p \cdot \delta\mathbf{r}\mathrm{d}\tau \tag{9}$$

Substituting equations (6)–(9) into equation (5) and using Green's theorem we can obtain

$$\begin{aligned} &\int_0^t \left[\rho \int_S \left(\ddot{U}_x x + \ddot{U}_y y + \ddot{U}_z z + \frac{\partial\phi}{\partial t} + \frac{1}{2}\nabla\phi \cdot \nabla\phi + g\eta + \frac{p}{\rho} \right) \right. \\ &\left. \times \delta\eta \mathrm{d}S + \left(M\ddot{\mathbf{U}} + \frac{\mathrm{d}\mathbf{Q}}{\mathrm{d}t} \right)\delta\mathbf{U} \right] \mathrm{d}t = 0 \end{aligned} \tag{10}$$

Due to the independence of U and η, the coupling dynamic equations of the system can be obtained as

$$\begin{aligned} &\frac{\partial\phi}{\partial t} + \frac{1}{2}\left[\left(\frac{\partial\phi}{\partial x}\right)^2 + \left(\frac{\partial\phi}{\partial y}\right)^2 + \left(\frac{\partial\phi}{\partial z}\right)^2 \right] + g\eta + \frac{p_0}{\rho} \\ &= -\ddot{U}_x x - \ddot{U}_y y - \ddot{U}_z z (\mathrm{at} z = \eta) \\ &\quad M\ddot{\mathbf{U}} + \frac{\mathrm{d}\mathbf{Q}}{\mathrm{d}t} = 0 \end{aligned} \tag{11}$$

where p_0 is the pressure at the free surface.

The first part of equation (11) is known as Euler's energy equation for the fluid motion, and the second part is the momentum equation of the whole system.

2.2. Boundary conditions

The boundary conditions at the tank walls and bottom are given as

$$\frac{\partial\phi}{\partial x}\Big|_{x=\pm\frac{a}{2}} = 0, \quad \frac{\partial\phi}{\partial y}\Big|_{y=\pm\frac{b}{2}} = 0, \quad \frac{\partial\phi}{\partial z}|_{z=-h} = 0 \tag{12}$$

3. State space model

Now let's consider the control of 2D sloshing in a rectangular tank. Laplace's equation, which is also known as the equation of continuity, is then

$$\frac{\partial^2\phi(t,y,z)}{\partial y^2} + \frac{\partial^2\phi(t,y,z)}{\partial z^2} = 0 \tag{13}$$

Supposing that there is only horizontal excitation acting on the tank body, then the dynamic equation (11) of the system can be simplified as

$$\begin{aligned} &\frac{\partial\phi(t,y,z)}{\partial t} + \frac{1}{2}\left[\left(\frac{\partial\phi(t,y,z)}{\partial y}\right)^2 + \left(\frac{\partial\phi(t,y,z)}{\partial z}\right)^2 \right] \\ &+ g\eta(t,y) + \frac{p_0}{\rho} = -\ddot{U}_y y (\mathrm{at} z = \eta) \end{aligned} \tag{14}$$

The boundary conditions at the tank walls and bottom are given as

$$\begin{aligned} &\frac{\partial\phi(t,y,z)}{\partial y}\Big|_{y=\pm\frac{L}{2}} = 0 \\ &\frac{\partial\phi(t,y,z)}{\partial z}|_{z=-h} = 0 \end{aligned} \tag{15}$$

Using separation of variables (Venugopal and Bernstein, 1996), let

$$\phi(t,y,z) = Q(t)H_1(y)H_2(z) \tag{16}$$

Since $\phi(t, y, z)$ satisfies equations (13) and (15), the horizontal and vertical mode shapes can be obtained as

$$H_{1n}(y) = \sqrt{\frac{2}{L}}\cos\frac{n\pi(y+L/2)}{L}$$
$$H_{2n}(z) = \cosh\frac{n\pi(z+h)}{L} \tag{17}$$

which implies that

$$\phi(t, y, z) = \sum_{n=1}^{\infty} Q_n(t)\sqrt{\frac{2}{L}}\cos\frac{n\pi(y+L/2)}{L}\cosh\frac{n\pi(z+h)}{L} \tag{18}$$

Replacing z by $\eta(t, y)$, it follows from equation (14) that

$$\eta(t, y) = -\frac{1}{g}\left\{\frac{\partial\phi(t, y, \eta(t, y))}{\partial t} + \frac{1}{2}\left[\left(\frac{\partial\phi(t, y, \eta(t, y))}{\partial y}\right)^2 + \left(\frac{\partial\phi(t, y, \eta(t, y))}{\partial z}\right)^2\right] + \frac{p_0}{\rho} + \ddot{U}_y(t)\, y\right\} \tag{19}$$

From the definition of the velocity potential, it follows that

$$\dot{\eta}(t, y) = \frac{\partial\phi(t, y, \eta(t, y))}{\partial z} \tag{20}$$

Differentiating equation (19) with respect to time and neglecting the nonlinear terms $\frac{\partial^2\phi(t, y, \eta(t, y))}{\partial t\partial\eta}\dot{\eta}(t, y)$ and $\dot{\eta}\left[(t, y)\eta(t, y) + \frac{\partial\phi(t, y, \eta(t, y))}{\partial y}\frac{\partial^2\phi(t, y, \eta(t, y))}{\partial y\partial t}\right]$ leads to the approximation

$$\dot{\eta}(t, y) = -\frac{1}{g}\left(\frac{\partial^2\phi(t, y, \eta(t, y))}{\partial t^2} + \frac{\mathrm{d}\ddot{U}_y(t)}{\mathrm{d}t}y\right) \tag{21}$$

Substituting equation (8) into equation (9) yields

$$\frac{\partial\phi(t, y, \eta(t, y))}{\partial z} + \frac{1}{g}\left(\frac{\partial^2\phi(t, y, \eta(t, y))}{\partial t^2} + \frac{\mathrm{d}\ddot{U}_y(t)}{\mathrm{d}t}y\right) = 0 \tag{22}$$

Define the input (or control) as $u(t) = \ddot{U}_y(t)$. Substitute $\phi(t, y, z)$ given by equation (18) into equation (22) and we can get

$$\sum_{n=1}^{\infty}\frac{n\pi}{L}Q_n(t)\sqrt{\frac{2}{L}}\cos\frac{n\pi(y+L/2)}{L}\sinh\frac{n\pi(z+h)}{L} + \sum_{n=1}^{\infty}\frac{1}{g}\ddot{Q}_n(t)\sqrt{\frac{2}{L}}\cos\frac{n\pi(y+L/2)}{L}\cosh\frac{n\pi(z+h)}{L} = -\frac{1}{g}\dot{u}(t)\, y \tag{23}$$

Assuming the sloshing elevation is small and approximating $z=0$ at the surface of the fluid yields

$$\sum_{n=1}^{\infty}\frac{n\pi}{L}Q_n(t)\sqrt{\frac{2}{L}}\cos\frac{n\pi(y+L/2)}{L}\sinh\frac{n\pi h}{L} + \sum_{n=1}^{\infty}\frac{1}{g}\ddot{Q}_n(t)\sqrt{\frac{2}{L}}\cos\frac{n\pi(y+L/2)}{L}\cosh\frac{n\pi h}{L} = -\frac{1}{g}\dot{u}(t)\, y \tag{24}$$

Multiplying both sides in equation (24) by $H_{1i}(y) = \sqrt{\frac{2}{L}}\cos\frac{i\pi(y+L/2)}{L}$ and integrating over $-L/2 \le y \le L/2$ yields

$$\frac{i\pi}{L}Q_n(t)\sqrt{\frac{2}{L}}\sinh\frac{i\pi h}{L} + \frac{1}{g}\ddot{Q}_n(t)\cosh\frac{i\pi h}{L} = \alpha_i\dot{u}(t) \tag{25}$$

where $\alpha_i = \begin{cases} -\sqrt{\frac{2}{L}}\frac{2L^2}{i^2\pi^2 g} \text{ for } i \text{ is odd} \\ 0 \text{ for } i \text{ is even} \end{cases}$

Take the first r modes into consideration and set the state as $\tilde{x}_1 = [Q_1\ \dot{Q}_1\ Q_2\ \dot{Q}_2 \ldots Q_r\ \dot{Q}_r]^{\mathrm{T}}$ so that equation (25) can be written as

$$\dot{\tilde{x}}_1 = \tilde{A}\tilde{x}_1(t) + \tilde{B}\dot{u}(t) \tag{26}$$

where

$$\tilde{A} = \mathrm{diag}\left[\tilde{A}_1\tilde{A}_2\tilde{A}_3 \ldots \tilde{A}_r\right]$$
$$(\tilde{A}_i)_{2\times 2} = \begin{bmatrix} 0 & 1 \\ -g\frac{i\pi}{L}\tanh\left(\frac{i\pi h}{L}\right) & 0 \end{bmatrix},$$
$$\tilde{B} = \left[0\sqrt{\frac{2}{L}}\frac{2L^2}{\pi^2\cosh\frac{\pi h}{L}} \cdots \times 0\sqrt{\frac{2}{L}}\frac{2L^2}{(2k+1)^2\pi^2\cosh\frac{(2k+1)\pi h}{L}} \cdots\right]^{\mathrm{T}} \tag{27}$$

We define the output as the sloshing height at the monitor point $y = y_{mp}$ given by

$$\tilde{x}_2(t) = \eta(t, y_{mp}) \tag{28}$$

Integrating equation (21) with zero initial condition yields

$$\eta(t, y) = -\frac{1}{g}\left\{\frac{\partial\phi(t, y_{mp}, \eta(t, y_{mp}))}{\partial t} + u(t)\, y_{mp}\right\} \tag{29}$$

Substitute equation (18) into equation (29) to obtain

$$\eta(t, y) = -\frac{1}{g}\left\{\sum_{n=1}^{r}\dot{Q}_n(t)\sqrt{\frac{2}{L}}\cos\frac{n\pi(y_{mp}+L/2)}{L} \times \cosh\frac{n\pi h}{L} + u(t)\, y_{mp}\right\} \tag{30}$$

From equations (28) and (30) it follows that

$$\tilde{x}_2(t) = \tilde{C}\tilde{x}_1(t) + \tilde{D}u(t) \tag{31}$$

where

$$\begin{aligned}\tilde{C} = \frac{1}{g}\sqrt{\frac{2}{L}}\bigg[&0\cos\frac{\pi(2y_{mp}+L)}{2L}\cosh\frac{\pi h}{L}\dots\\ &\times 0\cos\frac{r\pi(2y_{mp}+L)}{2L}\cosh\frac{r\pi h}{L}\bigg]\ \tilde{D} = \frac{1}{g}y_{mp}\end{aligned} \tag{32}$$

Let $x_1(t) = \tilde{x}_1(t) - \tilde{B}u(t)$ and $x_2(t) = \tilde{x}_2(t)$, then the state space model for sloshing in tank is comprised as

$$\begin{aligned}\dot{x}_1(t) &= Ax_1(t) + Bu(t),\\ x_2(t) &= Cx_1(t) + Du(t)\end{aligned} \tag{33}$$

where $A = \tilde{A}, B = \tilde{A}\tilde{B}, C = \tilde{C}, \mathrm{D} = \tilde{C}\tilde{B} + \tilde{D}$.

4. Control law design

In this section we set $g = 9.8\mathrm{m/s}^2,\ L = 1\mathrm{m},\ h/L = 0.5$, and $y_{mp} = L/2$. In the structural dynamic analysis of continuum, the number of degrees of freedom is quite large, which will result in massive and dense vibration modes. According to the actual calculation experience:

1. Because of the positive and negative alternation, there exists a lot of zero nodes displacement in high order modes;
2. The natural vibration frequency of the high-order mode is high, and since the displacement response is inversely proportional to the square of the natural frequency of the vibration, the displacement response of the high-order mode is small;
3. High order modes are not easy to be excited; usually only a few lower modes will be excited, so under normal circumstances, the structural vibration state can be expressed by modal superposition of only several low frequencies.

First three modes are what we care about, which means $r = 3$. Then

$$\tilde{A} = -g\pi\begin{bmatrix} 0 & 1 & 0 & 0 & 0 & 0\\ \tanh(\frac{\pi}{2}) & 0 & 0 & 0 & 0 & 0\\ 0 & 0 & 0 & 1 & 0 & 0\\ 0 & 0 & 2\tanh(\pi) & 0 & 0 & 0\\ 0 & 0 & 0 & 0 & 0 & 1\\ 0 & 0 & 0 & 0 & 3\tanh(\frac{3}{2}\pi) & 0 \end{bmatrix}$$

$$\tilde{B} = 2\sqrt{2}\left[0\ \frac{1}{\pi^2\cosh\frac{\pi}{2}}\ 0\ 0\ 0\ \frac{1}{9\pi^2\cosh\frac{3\pi}{2}}\right]^{\mathrm{T}},$$

$$\tilde{C} = \frac{\sqrt{2}}{g}\left[0\ -\cosh\frac{\pi}{2}\ 0\ \cosh\pi\ 0\ -\cosh\frac{3\pi}{2}\right],\quad \tilde{D} = \frac{1}{2g}$$

It can be noted that the external input can only affect the odd-number modes of sloshing. So we separate the first and third modes from the second one.

Here is how we deal with the first three modes of the sloshing. The system that consists of the first and third modes turns out to be controllable and observable. When we apply pole placement method to design the feedback controller, the second mode is out of consideration, which means the dimension of system state is four. Since the second mode of sloshing may also cause some unstable vibration, however, when we do simulation of the sloshing response to external excitations, we parallel the former system with that of the second mode. Simulation results in the next section show that the second mode cannot be excited and only the initial condition of this mode can cause difference in system response.

Since there exists unmodeled dynamics in the model, and there is a nonmatching uncertainty or disturbance in high-order modes, which inevitably will bring uncertainty, we need to control the impact of liquid sloshing with the desired accuracy under the uncertain conditions. Therefore, we propose a robust H infinity guaranteed cost control law in this section, which is a very suitable method for robust control with uncertainty and given quadratic performance index.

The system equation in a form of uncertainty is

$$\begin{cases}\dot{x} = (A + E\Delta_1 F)x + (B + M\Delta_2 N)u\,,\\ y = Cx\end{cases} \tag{34}$$

where Δ_1, Δ_2 are diagonal uncertainty matrices which satisfy $\Delta_1\Delta_1^T \le I, \Delta_2\Delta_2^T \le I$. E, F, M and N are corresponding weighting matrices.

Consider the uncertain system of equation (34). If there exist a control law u^* and a positive scalar J^* such that for all admissible uncertainties, the closed-loop system is stable and the closed-loop value of the cost function J satisfies $J \le J^*$, then J^* is said to be a guaranteed cost and u^* is said to be a guaranteed cost control law for the uncertain system of equation (34) (Li, 2000).

For the stability of the above system, the following results can be obtained:

Theorem 1. If there exist diagonal matrices $\Lambda > 0, \Theta > 0$, symmetric matrix $X = X^T > 0$ and matrix K that satisfies the inequality

$$\begin{aligned}&XA + A^TX + XBK + K^TB^TX + C^TQC + XE\Lambda E^TX\\&\quad + F^T\Lambda^{-1}F + XM\Theta M^TX + K^TN^T\Theta^{-1}NK + K^TRK \le 0\end{aligned}$$

then, under the controller

$$u = Kx \tag{35}$$

(i) The quadratic performance index satisfies

$$J = \int_0^{+\infty} (y^T(t)Qy(t) + u^T(t)Ru(t))\mathrm{d}t \le x_0^TXx_0 \tag{36}$$

where Q and R are positive definite weighting matrices.

(ii) The above uncertain system (equation (34)) has robust stability and satisfies the following H infinite norm constraints

$$\left\| \begin{pmatrix} Q^{\frac{1}{2}}C \\ R^{\frac{1}{2}}K \\ \Lambda^{-\frac{1}{2}}F \\ \Theta^{-\frac{1}{2}}NK \end{pmatrix} (sI - A - BK)^{-1}\left(E\Lambda^{\frac{1}{2}} \quad M\Theta^{\frac{1}{2}}\right) \right\|_\infty \le 1 \tag{37}$$

Proof.

(i) Let $P = X^{-1}, Y = KP$, then the above inequality can be changed into the following matrix inequality:

$$\begin{pmatrix} \Pi & Y^TN^T & Y^T & PC^T & PF^T \\ NY & -\Theta & 0 & 0 & 0 \\ Y & 0 & -R^{-1} & 0 & 0 \\ CP & 0 & 0 & -Q^{-1} & 0 \\ FP & 0 & 0 & 0 & -\Lambda \end{pmatrix} \le 0 \tag{38}$$

where $\Pi = AP + PA^T + BY + Y^TB^T + E\Lambda E^T + M\Theta M^T$. If there exist $\Lambda > 0, \Theta > 0$ that satisfy the linear matrix inequity (equation (38)), the following similarity transformation matrix is used,

$$T = \begin{bmatrix} X & 0 & 0 & 0 \\ 0 & I & 0 & 0 \\ 0 & 0 & I & 0 \\ 0 & 0 & 0 & I \end{bmatrix}$$

where $X = P^{-1}$. The inequality in equation (38) is equivalent to

$$\begin{bmatrix} \Pi & K^TN^T & K^T & C^T & F^T \\ NK & -\Theta & 0 & 0 & 0 \\ K & 0 & -R^{-1} & 0 & 0 \\ C & 0 & 0 & -Q^{-1} & 0 \\ F & 0 & 0 & 0 & -\Lambda \end{bmatrix} \le 0 \tag{39}$$

where $\Pi = XA + A^TX + XBK + K^TB^TX + XE\Lambda E^TX + XM\Theta M^TX$. According to the Schur complement lemma, the inequality of equation (39) is equivalent to inequality

$$\begin{aligned}&XA + A^TX + XBK + K^TB^TX + C^TQC + XE\Lambda E^TX\\&\quad + F^T\Lambda^{-1}F + XM\Theta M^TX + K^TN^T\Theta^{-1}NK\\&\quad + K^TRK \le 0\end{aligned} \tag{40}$$

It is obvious that

$$\begin{aligned}&\left(\Lambda^{\frac{1}{2}}\Delta_1^{\frac{1}{2}}E^{\mathrm{T}}X - \Lambda^{-\frac{1}{2}}\Delta_1^{\frac{1}{2}}F\right)^{\mathrm{T}}\\&\quad\times\left(\Lambda^{\frac{1}{2}}\Delta_1^{\frac{1}{2}}E^{\mathrm{T}}X - \Lambda^{-\frac{1}{2}}\Delta_1^{\frac{1}{2}}F\right) \ge 0\end{aligned}$$

which is also can be written as

$$\begin{aligned}&XE\left(\Delta_1^{\frac{1}{2}}\right)^{\mathrm{T}}\Lambda\Delta_1^{\frac{1}{2}}E^{\mathrm{T}}X + F^{\mathrm{T}}\left(\Delta_1^{\frac{1}{2}}\right)^{\mathrm{T}}\Lambda^{-1}\Delta_1^{\frac{1}{2}}F\\&\quad\ge F^{\mathrm{T}}\Delta_1E^{\mathrm{T}}X + XE\Delta_1F\end{aligned} \tag{41}$$

Since $\Delta_1^{\mathrm{T}}\Delta_1 \le I$, then $(\Delta_1^{\frac{1}{2}})^{\mathrm{T}}\Delta_1^{\frac{1}{2}} \le I$, so $(\Delta_1^{\frac{1}{2}})^{\mathrm{T}}\Lambda\Delta_1^{\frac{1}{2}} \le \Lambda$. Substitute into the inequity of equation (41) to yield

$$XE\Lambda E^{\mathrm{T}}X + F^{\mathrm{T}}\Lambda^{-1}F \ge F^{\mathrm{T}}\Delta_1E^{\mathrm{T}}X + XE\Delta_1F \tag{42}$$

Similarly, under the precondition that $\Delta_2^T\Delta_2 \le I$, the following inequity can be obtained

$$\begin{aligned}&XM\Delta_2NK + K^TN^T\Delta_2^TM^TX\\&\quad\le XM\Theta M^TX + K^TN^T\Theta^{-1}NK\end{aligned} \tag{43}$$

Combined with the inequalities of equations (42) and (43), if the inequality of equation (40) holds, then the following inequality can be obtained

$$\begin{aligned}&XA + A^TX + XBK + K^TB^TX + C^TQC + XE\Delta_1F\\&\quad + F^T\Delta_1^TE^TX + XM\Delta_2NK + K^TN^T\Delta_2^TM^TX\\&\quad + K^TRK \le 0\end{aligned} \tag{44}$$

We define the Lyapunov function as $V(t) = x^T X x$, where $X > 0$. Then

$$\begin{aligned}\dot{V}(t) = x^{\mathrm{T}}(XA + XE\Delta_1 F + XBK + XM\Delta_2 NK)x \\ + x^{\mathrm{T}}(A^{\mathrm{T}}X + F^{\mathrm{T}}\Delta_1^{\mathrm{T}}E^{\mathrm{T}}X + K^{\mathrm{T}}B^{\mathrm{T}}X \\ + K^{\mathrm{T}}N^{\mathrm{T}}\Delta_2^{\mathrm{T}}M^{\mathrm{T}}X)x\end{aligned} \tag{45}$$

If the inequality of equation (44) holds, then the following inequality can be established

$$\begin{aligned}x^T(XA + A^TX + XBK + K^TB^TX)x \\ + x^T(C^TQC + XE\Delta_1 F + F^T\Delta_1^TE^TX)x \\ + x^T(XM\Delta_2 NK + K^TN^T\Delta_2^TM^TX + K^TRK)x \le 0\end{aligned} \tag{46}$$

Substituting equation (45) into equation (46) yields

$$\dot{V}(t) \le -x^{\mathrm{T}}(CQC + KRK)x = -(y^{\mathrm{T}}Qy + u^{\mathrm{T}}Ru) < 0 \tag{47}$$

and $V(\infty) = 0$. The integral of the inequality of equation (47) is given as

$$V(\infty) - V(0) \le -\int_0^{\infty} \left(y^T(t)Qy(t) + u^T(t)Ru(t)\right)\mathrm{d}t \tag{48}$$

i.e.

$$\int_0^{+\infty} (y^T(t)Qy(t) + u^T(t)Ru(t))\mathrm{d}t \le V(0) = x_0^TXx_0 \tag{49}$$

(ii) From the inequity of equation (44), it can be obtained that

$$\begin{aligned}X(A + E\Delta_1 F + (B + M\Delta_2 N)K) + (A + E\Delta_1 F \\ + (B + M\Delta_2 N)K)^TX + C^TQC + K^TRK \le 0\end{aligned}$$

from which it can be noted that $A + E\Delta_1 F + (B + M\Delta_2 N)K$ is robust and stable. The inequality (40) can be rewritten as

$$\begin{aligned}X(A + BK) + (A^T + K^TB^T)X + X(E\Lambda E^T + M\Theta M^T)X \\ + C^TQC + K^TRK + F^T\Lambda^{-1}F + K^TN^T\Theta^{-1}NK \le 0\end{aligned} \tag{50}$$

Let $\bar{A} = A + BK$, $\bar{B} = E\Lambda^{\frac{1}{2}}M\Theta^{\frac{1}{2}}$ and $\bar{C} = \begin{pmatrix} Q^{\frac{1}{2}}C \\ R^{\frac{1}{2}}K \\ \Lambda^{-\frac{1}{2}}F \\ \Theta^{-\frac{1}{2}}NK \end{pmatrix}$, then the inequality of equation (50) can be expressed by

$$X\bar{A} + \bar{A}^TX + X\bar{B}\bar{B}^TX + \bar{C}^T\bar{C} \le 0,$$

which reveals that the system $\begin{cases} \dot{x} = \bar{A}x + \bar{B}u \\ y = \bar{C}x \end{cases}$ satisfies the H infinite norm condition $\left\|\bar{C}(sI - \bar{A})^{-1}\bar{B}\right\|_{\infty} \le 1$.

The stable system represented by the inequality of equation (50) covers the uncertainty range of the original uncertain system (equation (34)), so the original uncertain system (equation (34)) meets the robust stability of the closed-loop condition of equation (37). That is, the controller design method not only considers the quadratic performance constraints, but it also covers the H infinite norm constraints, so the designed controller has good robustness and we finish the proof of Theorem 1.

In the Theorem 1, we can add the pole placement constraints of the system, such as $A + \alpha I$ to replace A. When the corresponding matrix inequalities hold, the corresponding real eigenvalues of the closed-loop system are smaller than $-\alpha$.

5. Simulation results

In this section, we present the results of simulation using the proposed method and make comparison with traditional LQR control.

Assuming the first mode, which has the greatest impact on the whole sloshing dynamic behavior, has an error coefficient of $\pm 10\%$, i.e.

$$E = 0.1 \times \begin{bmatrix} A_{11} & A_{12} & A_{13} & A_{14} \\ A_{21} & A_{22} & A_{23} & A_{24} \\ 0 & 0 & 0 & 0 \\ 0 & 0 & 0 & 0 \end{bmatrix},$$

$$F = I, \quad M = 0.1 \times \begin{bmatrix} B_{11} \\ 0 \\ 0 \\ 0 \end{bmatrix}, \quad N = I$$

We are designing a robust controller to make the wave height of sloshing come to zero. The weighing matrices are chosen as $Q = CC^{\mathrm{T}}$ and $R = I$. Standard LQR design with output weighting is to minimize $J(u) = \int_0^{\infty} (y^{\mathrm{T}}Qy + u^{\mathrm{T}}Ru)\mathrm{d}t$. The weighing matrices are also chosen as $Q = CC^{\mathrm{T}}$ and $R = I$.

The impulse responses of wave height with respective controller based on standard LQR and robust H infinite guaranteed cost control are shown in Figure 2. The overshoot of robust H infinite guaranteed cost control is 0.087 m, while the overshoot of standard LQR

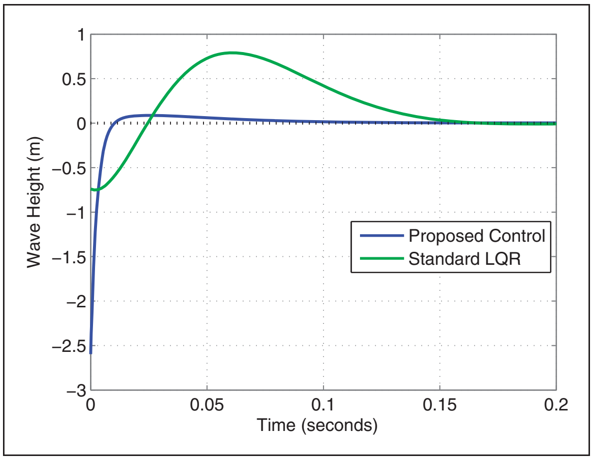

Figure 2. Impulse response under robust H infinite guaranteed cost control and standard LQR control.

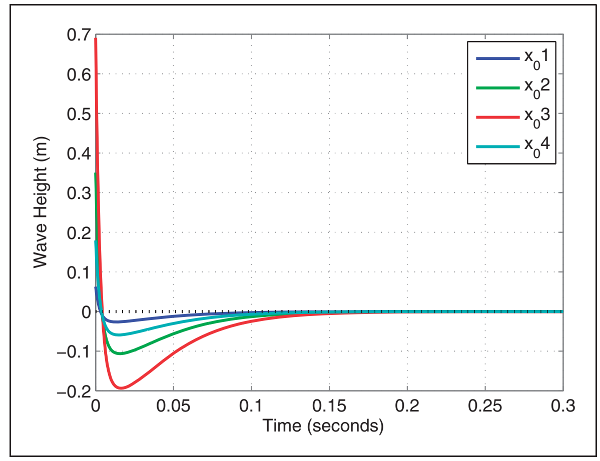

Figure 4. Response to different initial conditions of robust H infinite guaranteed cost control.

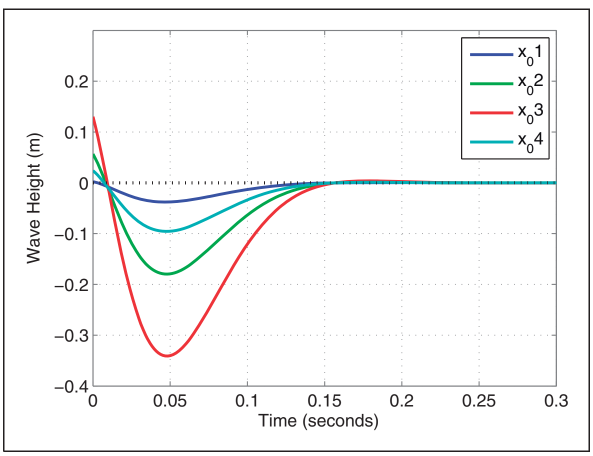

Figure 3. Response to different initial conditions of standard LQR.

control is 0.790 m. It can be also seen that for the proposed robust guaranteed cost control, both the rise time and convergence time are much shorter than those of standard LQR control.

Figures 3 and 4 give the response to different initial conditions of standard LQR and robust H infinite guaranteed cost control, respectively. It can be clearly seen that the sloshing intensity can be attenuated more quickly by control based on the proposed control than that of standard LQR under the same conditions.

Figure 5 gives the comparison between control inputs of robust H infinite guaranteed cost control and standard LQR that are required to achieve sloshing-attenuating under same initial conditions. It can be noted in Figure 5(a) that although the required control input of the proposed control is larger in the beginning, it quickly comes to zero. One can see from Figure 5(b) that it almost takes twice as long as that of robust H

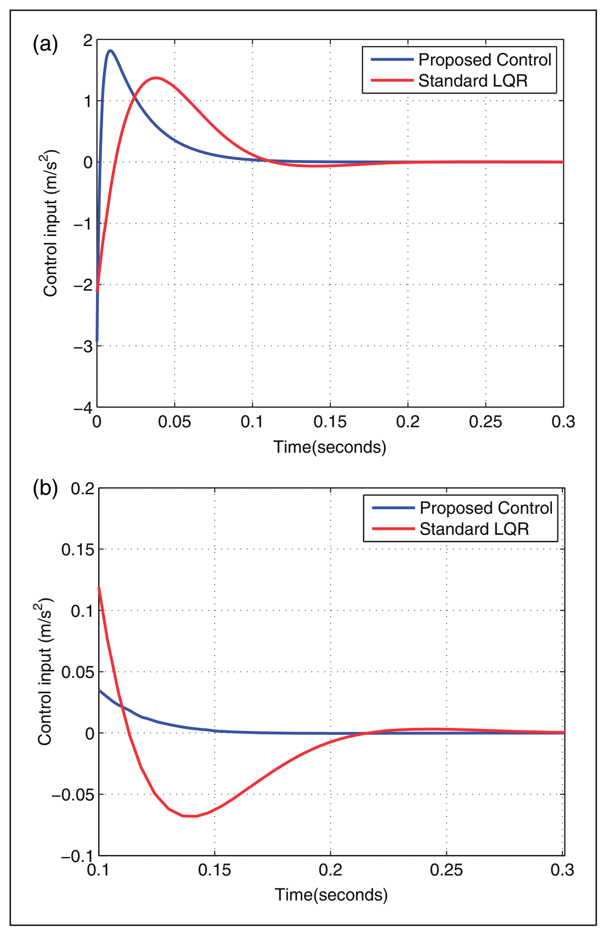

Figure 5. Comparison of control input under same conditions: (a) whole process comparison; (b) local time comparison.

infinite guaranteed cost control (0.15 s) for the traditional LQR (0.30 s) to make the system stable.

6. Conclusion

In this paper, the nonlinear fluid dynamics modeling and linear optimization control are combined, by which the problem of modeling and control of sloshing is solved effectively. There are many practical applications, such as the use of momentum reaction to achieve the stability of liquid filled satellite.

This paper focuses on how to establish the nonlinear dynamic equations describing the fluid motion by the Lagrange Hamilton method. Based on the analysis of the influence of the vibration mode on the dynamic characteristics of the fluid, the main feature of the model is extracted and a linearization model for control is established. The optimal pole assignment based on the performance requirements and the robust H infinite guaranteed cost control method which can adapt to the uncertainties and ensure the control performance are given. The simulation results show that the nonlinear dynamic modeling and linear optimal control method presented in this paper has good adaptability and controllability to the sloshing system.

Since the state we have defined before has no specific physical meaning, it is difficult to know the whole information of the state, for which the state observer is needed in order to realize the state feedback control. In our future work, the uncertainty of the state observer will be considered, and also the linearization of 3D dynamic equation will be investigated with a hope to provide support for further application in industry and engineering.

Declaration of Conflicting Interests

The author(s) declared no potential conflicts of interest with respect to the research, authorship, and/or publication of this article.

Funding

The author(s) disclosed receipt of the following financial support for the research, authorship, and/or publication of this article: This research was supported by the National Natural Science Foundation of China under Grant No. 11332001 and 61773024, Research project fund 17-163-11-ZT-003-018-01, Joint fund of the Ministry of education of China (6141A020223).

ORCID iD

Tingting Zhang http://orcid.org/0000-0002-2693-2979

References

Abramson HN (1966) *The dynamics of liquids in moving containers*. Report SP 106. Washington, DC: NASA.

Bandyopadhyay B, Gandhi PS and Kurode S (2009) Sliding mode observer based sliding mode controller for slosh-free motion through PID scheme. *IEEE Transactions on Industrial Electronics* 56(9): 3432–3442.

Chen K, Li J and Wang T (2005) Nonlinear dynamics modeling and analysis of liquid sloshing in rectangular tank. *Acta Mechanica Sinica* 37(3): 339–345.

De Souza AG and de Souza LCG (2014) Satellite attitude control system design taking into account the fuel slosh and flexible dynamics. *Mathematical Problems in Engineering* 2014(1): 1–8.

Ferrant P and Le Touze D (2001) Simulation of sloshing waves in a 3D tank based on a pseudo-spectral method. In: *Proceedings of the 16th international workshop on water waves and floating bodies*, Hiroshima, Japan, 22–25 April 2001.

Li Y (2000) Optimal guaranteed cost control of linear uncertain systems: an LMI approach. *Control Theory and Applications* 17(3): 423–428.

Liu Y (2015) A survey of approaches in dynamics of rigid body containing liquid. *Mechanics in Engineering* 37(3): 397–400.

Love JS and Tait MJ (2014) Equivalent mechanical model for tuned liquid damper of complex tank geometry coupled to a 2D structure. *Structural Control & Health Monitoring* 21(1): 43–60.

Takashi I, Raouf AI, Yuji H, et al. (2012) Nonlinear liquid sloshing in a square tank subjected to obliquely horizontal excitation. *Journal of Fluid Mechanics* 700: 304–328.

Telste JG (1985) Calculation of fluid motion resulting from large amplitude forced heave motion of a two-dimensional cylinder in a free surface. In: *Proceedings of the fourth international conference on numerical ship hydrodynamics*, Washington, DC, 24–27 September 1985, paper no. 81C93.

Venugopal R and Bernstein DS (1996) State space modeling and active control of slosh. *IEEE international conference on control applications*, Dearborn, MI, 15–18 September 1996, pp.1072-1077. New York: IEEE.

Yue B (2005) Three-dimensional large amplitude liquid sloshing under pitching excitations. *Acta Mechanica Sinica* 37(2): 199–203.

Zan Q and Huang J (2015) Dynamics and control of three-dimensional slosh in a moving rectangular liquid container undergoing planar excitations. *IEEE Transactions on Industrial Electronics* 62(4): 2309–2318.